
Article:
Chen, H., Hou, C., Zhu, W.P. et al. (4 more authors) (2017) ESPRIT-like two-dimensional direction finding for mixed circular and strictly noncircular sources based on joint diagonalization. Signal Processing, 141. pp. 48-56. ISSN 0165-1684

https://doi.org/10.1016/j.sigpro.2017.05.024

ESPRIT-like Two-dimensional Direction Finding for Mixed Circular and Strictly Noncircular Sources Based on Joint Diagonalization

Hua Chen[a], Chunping Hou[a], Wei-Ping Zhu[b], Wei Liu[c], Yang-Yang Dong[d], Qing Wang[a]

[a]*School of Electronic Informatin Engineering, Tianjin University, Tianjin 300072, P. R. China.*
[b]*Department of Electrical and Computer Engineering, Concordia University, Montreal, QC H3G 1M8, Canada.*
[c]*Department of Electronic and Electrical Engineering, University of Sheffield, Sheffield S1 3JD, UK.*
[d]*Key Laboratory of Electronic Information Countermeasure and Simulation Technology, Ministry of Education, Xidian University, Xian 710071, Shanxi, P. R. China.*

Abstract

In this paper, a two-dimensional (2-D) direction-of-arrival (DOA) estimation method for a mixture of circular and strictly noncircular signals is presented based on a uniform rectangular array (URA). We first formulate a new 2-D array model for such a mixture of signals, and then utilize the observed data coupled with its conjugate counterparts to construct a new data vector and its associated covariance matrix for DOA estimation. By exploiting the second-order non-circularity of incoming signals, a computationally effective ESPRIT-like method is adopted to estimate the 2-D DOAs of mixed sources which are automatically paired by joint diagonalization of two direc-

*Corresponding author
Email addresses: dkchenhua@tju.edu.cn (Hua Chen), weiping@ece.concordia.ca (Wei-Ping Zhu), w.liu@sheffield.ac.uk (Wei Liu), dongyangyang2104@126.com (Yang-Yang Dong), wqelaine@tju.edu.cn (Qing Wang)

tion matrices. One particular advantage of the proposed method is that it can solve the angle ambiguity problem when multiple incoming signals have the same angle θ or β. Furthermore, the theoretical error performance of the proposed method is analyzed and a closed-form expression for the deterministic Cramer-Rao bound (CRB) for the considered signal scenario is derived. Simulation results are provided to verify the effectiveness of the proposed method.
Keywords:
Two-dimensional (2-D), direction of arrival (DOA), noncircular signal, uniform rectangular array (URA), joint diagonalization, angle ambiguity.

---

1. Introduction

Direction-of-arrival (DOA) plays a significant role in the area of array signal processing [1, 2]. Recently, the second-order non-circularity of incoming signals has been exploited in both one dimensional (1-D) [3–8] and two-dimensional (2-D) or multi-dimensional [9–15] DOA estimation. However, the algorithms developed thus far only consider strictly noncircular incoming signals. In practice, a more realistic case is a mixture of circular (e.g. quadrature phase shift keying, QPSK) and strictly non-circular (e.g. binary phase shift keying, BPSK) signals.

There have been several approaches for joint estimation of circular and strictly noncircular signals in 1-D direction finding. In [16], a new data vector containing both the original data and the conjugate version was proposed to form two estimators for strictly noncircular and circular signals, respectively. Then in [17], an improved algorithm was developed for estimating the

DOAs of strictly noncircular and circular signals separately by exploiting the circularity difference between the two classes of signals. However, all these algorithms require the computationally expensive peak search of the MUSIC pseudo spectrum. Recently, an ESPRIT-based parameter estimation algorithm was developed in [18] for the above case, where a closed-form expression related to strictly noncircular and circular signals was derived for efficient 1-D DOA estimation. In addition, in [19], a sparse representation algorithm for mixed signals was proposed, where overcomplete dictionaries were exploited subject to sparsity constraints to jointly represent the covariance and elliptic covariance matrices of the array output. For the 2-D case, to our best knowledge, the only work on joint direction estimation of circular and noncircular signals was reported in [20] where four 1-D peak searching estimators were constructed using two parallel uniform linear arrays (ULAs) along with a computationally expensive MUSIC method. Besides, the method in [20] can not solve the angle ambiguity problem when multiple incoming signals have the same angle θ or β, and the theoretical performance analysis is not mentioned in [20]. More recently, an ESPRIT based method was proposed in [21] to estimate 2-D angle parameters for bistatic MIMO radar using a joint diagonalization algorithm. However, no noncircularity information is considered in the formulation. Yang [22] proposed an ESPRIT algorithm for coexistence of noncircular and circular sources in bistatic MIMO radar, but it can not solve the angle ambiguity problem when multiple incoming signals have the same angle θ or β. In addition, it needs additional procedure to pair the 2-D angle parameters.

Inspired by the simultaneous diagonalization idea in [21], we propose

in this paper a method to deal with the 2-D DOA estimation problem in the presence of a mixture of circular and strictly noncircular signals. Our method utilizes a uniform rectangular array (URA) and an ESPRIT-like 2-D DOA estimation algorithm to exploit the non-circularity information of the impinging signals. By building a general 2-D array model with mixed circular and strictly noncircular signals, we first construct a new data vector and its associated covariance matrix by exploiting the observed array data coupled with its conjugate counterpart. Then, an efficient ESPRIT-like method is developed to estimate the 2-D DOA of the mixed sources, where the angle θ or β are paired automatically, and meanwhile the angle ambiguity problem of angle θ or β is settled, by joint diagonalization of two direction matrices. Finally, the theoretical error performance of the proposed method is analyzed and a closed-form expression for the deterministic Cramer-Rao bound (CRB) for the mixed signals scenario is derived.

Throughout the paper, the notations $(\cdot)^*$, $(\cdot)^T$, $(\cdot)^{-1}$, $(\cdot)^+$, and $(\cdot)^H$ represent conjugation, transpose, inverse, pseudo-inverse, and conjugate transpose, respectively. $E(\cdot)$ is the expectation operation; diag$(\cdot)$ stands for the diagonalization operation; $\mathbf{I}_p$ denotes the p-dimensional identity matrix; $blkdiag(\mathbf{Z}_1, \mathbf{Z}_2)$ represents a block diagonal matrix with diagonal entries $\mathbf{Z}_1$ and $\mathbf{Z}_2$; the $p \times p$ matrix $\mathbf{\Upsilon}_p$ denotes an exchange matrix with ones on its anti-diagonal and zeros elsewhere; $\otimes$ is the kronecker matrix product operation; $arg(\cdot)$ is the phase; Re$(\cdot)$ and Im$(\cdot)$ denote the real and imaginary part; $\mathbf{e}_i$ denotes the ith column of the identity matrix; $tr(\cdot)$ denotes the trace of a matrix.

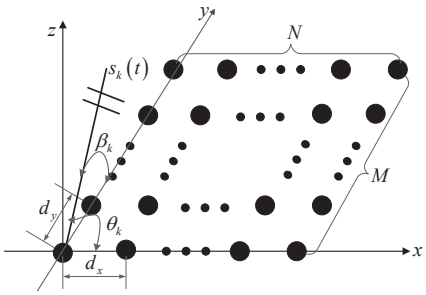

Fig. 1: Geometry of a URA

2. Array model

Consider $K = K_n + K_c$ (assume the number of mixed signals is known) uncorrelated far-field sources that are a mixture of K_n strictly noncircular sources $s_{n,k}(t)$ and K_c circular sources $s_{c,k}(t)$ with identical wavelength λ. They impinge on to an URA of $M \times N$ omnidirectional sensors spaced by d_x in each row and d_y in each column, as shown in Fig.1.

The direction of the kth signal is denoted as $(\theta_k, \beta_k), k = 1, 2, \ldots, K$. Thus, the output of the array at time t can be modeled as

$$\mathbf{x}(t) = \mathbf{A}\mathbf{s}(t) + \mathbf{n}(t) \tag{1}$$

where $\mathbf{x}(t) = [x_1(t), \cdots, x_N(t), x_{N+1}(t), \cdots, x_{2N}(t), \cdots, x_{MN}(t)]^{\mathrm{T}}$ is composed of the MN received array signals, $\mathbf{A} = [\mathbf{a}(\theta_1, \beta_1), \mathbf{a}(\theta_2, \beta_2), \cdots, \mathbf{a}(\theta_K, \beta_K)]^T$ is the array manifold matrix, $\mathbf{s}(t) = [s_1(t), s_2(t), \cdots, s_K(t)]^T$ is the source signal vector and $\mathbf{n}(t) = [n_1(t), \cdots, n_N(t), n_{N+1}(t), \cdots, n_{2N}(t), \cdots, n_{MN}(t)]^T$ is the additive white Gaussian complex circular noise vector with its elements being of zero mean and variance σ^2. The steering vector $\mathbf{a}(\theta_k, \beta_k)$ is given by

$$\mathbf{a}(\theta_k, \beta_k) = \mathbf{a}_y(\beta_k) \otimes \mathbf{a}_x(\theta_k) \tag{2}$$

where

$$\mathbf{a}_y(\beta_k) = [1, \varphi_y(\beta_k), \cdots {\varphi_y}^{M-1}(\beta_k)]^T \tag{3}$$

$$\mathbf{a}_x(\theta_k) = [1, \varphi_x(\theta_k), \cdots {\varphi_x}^{N-1}(\theta_k)]^T \tag{4}$$

with

$$\varphi_y(\beta_k) = \exp\{j2\pi\lambda^{-1}d_y \cos(\beta_k)\} \tag{5}$$

$$\varphi_x(\theta_k) = \exp\{j2\pi\lambda^{-1}d_x \cos(\theta_k)\} \tag{6}$$

As in [18], we decompose each of the circular sources into two uncorrelated strictly non-circular sources with the same DOA. Without loss of generality, let the first K_n elements in $\mathbf{s}(t)$ represent the strictly non-circular signals. Thus, $\mathbf{s}(t)$ can be represented as

$$\mathbf{s}(t) = \begin{bmatrix} \mathbf{\Psi} & \mathbf{0} & \mathbf{0} \\ \mathbf{0} & \mathbf{I}_{K_c} & j\mathbf{I}_{K_c} \end{bmatrix} \begin{bmatrix} \mathbf{s}_n(t) \\ \mathbf{s}_c^r(t) \\ \mathbf{s}_c^q(t) \end{bmatrix} = \mathbf{\Psi_1}\tilde{\mathbf{s}}(t) \tag{7}$$

where $\mathbf{\Psi} = diag(e^{j\phi_1}, \ldots, e^{j\phi_{K_n}})$ represents the rotation phases corresponding to the strictly non-circular sources. Furthermore, $\mathbf{\Psi_1}$ is of size $K \times K'$ with $K' = K_n + 2K_c$ and the real-valued $K' \times 1$ vector $\tilde{\mathbf{s}}(t)$ contains the symbols of the K_n strictly non-circular sources $\mathbf{s}_n(t)$ as well as the K_c real parts $\mathbf{s}_c^r(t)$ and K_c imaginary parts $\mathbf{s}_c^q(t)$ of the circular signals $\mathbf{s}_c(t)$. The array manifold matrix $\mathbf{A}$ can be rewritten as

$$\mathbf{A} = [\mathbf{A}_n \quad \mathbf{A}_c] \tag{8}$$

where $\mathbf{A}_n$ and $\mathbf{A}_c$ denote the array manifold matrix related to strictly non-cirular and circular signals, respectively. Using (7), the observed data model

in (1) can be expressed as

$$\mathbf{x}(t) = \mathbf{A}\boldsymbol{\Psi}_{\mathbf{1}}\tilde{\mathbf{s}}(t) + \mathbf{n}(t) = \tilde{\mathbf{A}}\tilde{\mathbf{s}}(t) + \mathbf{n}(t) \tag{9}$$

where $\tilde{\mathbf{A}} = \mathbf{A}\boldsymbol{\Psi}_{\mathbf{1}}$ denotes the modified array manifold matrix.

For notional convenience, the indices of θ, β and t will be omitted in the following discussion while not causing confusion.

3. The Proposed Method

In order to take advantage of the strict non-circularity of the strictly non-circular sources and the virtual strict non-circularity of the circular sources, a new data vector is defined by stacking the original data and its conjugate counterpart as

$$\tilde{\mathbf{x}} = \begin{bmatrix} \mathbf{x} \\ \boldsymbol{\Upsilon}_{MN}\mathbf{x}^* \end{bmatrix} = \begin{bmatrix} \tilde{\mathbf{A}}\tilde{\mathbf{s}} \\ \boldsymbol{\Upsilon}_{MN}\tilde{\mathbf{A}}^*\tilde{\mathbf{s}}^* \end{bmatrix} + \begin{bmatrix} \mathbf{n} \\ \boldsymbol{\Upsilon}_{MN}\mathbf{n}^* \end{bmatrix} = \breve{\mathbf{A}}\tilde{\mathbf{s}} + \breve{\mathbf{n}} \tag{10}$$

where

$$\begin{aligned} \breve{\mathbf{A}} &= \begin{bmatrix} \tilde{\mathbf{A}} \\ \boldsymbol{\Upsilon}_{MN}\tilde{\mathbf{A}}^* \end{bmatrix} \\ &= \begin{bmatrix} \mathbf{A}_n\boldsymbol{\Psi} & \mathbf{A}_c \begin{bmatrix} \mathbf{I}_{K_c} & j\mathbf{I}_{K_c} \end{bmatrix} \\ \boldsymbol{\Upsilon}_{MN}\mathbf{A}_n^*\boldsymbol{\Psi}^* & \boldsymbol{\Upsilon}_{MN}\mathbf{A}_c^* \begin{bmatrix} \mathbf{I}_{K_c} & -j\mathbf{I}_{K_c} \end{bmatrix} \end{bmatrix} \end{aligned} \tag{11}$$

is the extended array manifold matrix of size $2MN \times K'$, $\breve{\mathbf{n}} = \begin{bmatrix} \mathbf{n} \\ \boldsymbol{\Upsilon}_{MN}\mathbf{n}^* \end{bmatrix}$ is the $2MN \times 1$ noise vector, and $\tilde{\mathbf{s}} = \tilde{\mathbf{s}}^*$. Then, the covariance matrix of $\tilde{\mathbf{x}}$ is given by

$$\mathbf{R} = E[\tilde{\mathbf{x}}\tilde{\mathbf{x}}^H] = \breve{\mathbf{A}}\mathbf{R}_s\breve{\mathbf{A}}^H + \sigma^2\mathbf{I}_{2MN} \tag{12}$$

where $\mathbf{R}_s = E[\tilde{\mathbf{s}}\tilde{\mathbf{s}}^H]$ is the covariance matrix of $\tilde{\mathbf{s}}$.

Remark 1: In practice, only a finite number of observed data is available. Thus, $\mathbf{R}$ has to be estimated by

$$\hat{\mathbf{R}} \approx \frac{1}{L}\sum_{l=1}^{L}\hat{\tilde{\mathbf{x}}}(l)\hat{\tilde{\mathbf{x}}}^{H}(l). \tag{13}$$

where L denotes the number of snapshots.

Since the mixed signals are not correlated with each other, we perform eigenvalue decomposition (EVD) of $\mathbf{R}$ as follows

$$\mathbf{R} = \mathbf{U}_s\mathbf{\Lambda}_s\mathbf{U}_s^H + \mathbf{U}_n\mathbf{\Lambda}_n\mathbf{U}_n^H \tag{14}$$

where the $2MN \times K'$ matrix $\mathbf{U}_s$ and the $2MN \times (2MN - K')$ matrix $\mathbf{U}_n$ are the signal subspace and noise subspace, respectively. The $K' \times K'$ matrix $\mathbf{\Lambda}_s = \text{diag}(\lambda_1,\lambda_2\cdots,\lambda_{K'})$ and the $(2MN - K') \times (2MN - K')$ matrix $\mathbf{\Lambda}_n = \text{diag}(\lambda_{K'+1},\lambda_{K'+2}\cdots,\lambda_{2MN})$ are corresponding diagonal matrices. $\lambda_1 \geq \lambda_2 \geq \cdots \geq \lambda_{K'} > \lambda_{K'+1} = \cdots = \lambda_{2MN} = \sigma^2$ are eigenvalues of $\mathbf{R}$. As $\breve{\mathbf{A}}$ and $\mathbf{U}_s$ span the same column space, there is a non-singular matrix $\mathbf{T}$ that satisfies $\breve{\mathbf{A}} = \mathbf{U}_s\mathbf{T}$.

Define a new matrix $\mathbf{E}_s$ as

$$\mathbf{E}_s = \mathbf{U}_s\mathbf{\Lambda}_s^{\frac{1}{2}}, \tag{15}$$

and four selection matrices as

$$\mathbf{J}_{1a} = [\mathbf{I}_{N-1}\ \mathbf{0}_{(N-1)\times 1}] \tag{16}$$

$$\mathbf{J}_{1b} = [\mathbf{0}_{(N-1)\times 1}\ \mathbf{I}_{N-1}] \tag{17}$$

$$\mathbf{J}_{2a} = [\mathbf{I}_{M-1}\ \mathbf{0}_{(M-1)\times 1}] \tag{18}$$

$$\mathbf{J}_{2b} = [\mathbf{0}_{(M-1)\times 1}\ \mathbf{I}_{M-1}] \tag{19}$$

Then, the selection matrices of 1-D DOA θ of the mixed strictly noncircular and circular sources can be expressed as

$$\mathbf{J}_1 = blkdiag(\mathbf{J'}_{1a}\ ,\ \boldsymbol{\Upsilon}_{M(N-1)}\mathbf{J'}_{1b}\boldsymbol{\Upsilon}_{MN}) \tag{20}$$

$$\mathbf{J}_2 = blkdiag(\mathbf{J'}_{1b}\ ,\ \boldsymbol{\Upsilon}_{M(N-1)}\mathbf{J'}_{1a}\boldsymbol{\Upsilon}_{MN}) \tag{21}$$

where $\mathbf{J'}_{1a} = \mathbf{I}_M \otimes \mathbf{J}_{1a}$ and $\mathbf{J'}_{1b} = \mathbf{I}_M \otimes \mathbf{J}_{1b}$.

As for the selection matrices of 1-D DOA β, we have

$$\mathbf{J}'_1 = blkdiag(\mathbf{J'}_{2a}\ ,\ \boldsymbol{\Upsilon}_{N(M-1)}\mathbf{J'}_{2b}\boldsymbol{\Upsilon}_{MN}) \tag{22}$$

$$\mathbf{J}'_2 = blkdiag(\mathbf{J'}_{2b}\ ,\ \boldsymbol{\Upsilon}_{N(M-1)}\mathbf{J'}_{2a}\boldsymbol{\Upsilon}_{MN}) \tag{23}$$

where $\mathbf{J'}_{2a} = \mathbf{J}_{2a} \otimes \mathbf{I}_N$ and $\mathbf{J'}_{2b} = \mathbf{J}_{2b} \otimes \mathbf{I}_N$.

Next, we define two direction matrices related to θ and β as follows

$$\boldsymbol{\Omega}_\theta = (\mathbf{J}_1\mathbf{E}_s)^+(\mathbf{J}_2\mathbf{E}_s) \tag{24}$$

$$\boldsymbol{\Omega}_\beta = (\mathbf{J}'_1\mathbf{E}_s)^+(\mathbf{J}'_2\mathbf{E}_s) \tag{25}$$

It is noticed that in [22], the EVD of $\boldsymbol{\Omega}_\theta$ and $\boldsymbol{\Omega}_\beta$ is performed independently as

$$\boldsymbol{\Omega}_\theta = \mathbf{U}_\theta\boldsymbol{\Theta}_\theta\mathbf{U}_\theta^H \tag{26}$$

$$\boldsymbol{\Omega}_\beta = \mathbf{U}_\beta\boldsymbol{\Theta}_\beta\mathbf{U}_\beta^H \tag{27}$$

where $\mathbf{U}_\theta$ and $\mathbf{U}_\beta$ are the $K' \times K'$ unitary matrices, $\boldsymbol{\Theta}_\theta$ and $\boldsymbol{\Theta}_\beta$ are the eigenvalue matrices that correspond to θ and β, respectively. It should be pointed out that performing EVD of (26) and (27) separately, would lead to the pairing problem between θ and β. Also, there are two identical eigenvalues for the same circular source both in (26) and (27) since we have virtually

decomposed each circular source into two uncorrelated strictly non-circular sources with the same DOA. This may cause rank-loss problem in (26) and (27). Moreover, if the same θ or β exists in the incoming mixed signals, the eigenvalue spectrum in (26) and (27) may degenerate.

In order to solve the above three problems, we now apply the joint diagonalization method as used in blind signal separation [23] to the two direction matrices $\mathbf{\Omega}_\theta$ and $\mathbf{\Omega}_\beta$ rather than perform EVD of $\mathbf{\Omega}_\theta$ and $\mathbf{\Omega}_\beta$. Analogous to [21], it can be easily deduced that

$$\mathbf{\Omega}_\theta = (\mathbf{J}_1\mathbf{E}_s)^+(\mathbf{J}_2\mathbf{E}_s) = \mathbf{U}\mathbf{\Theta}_\theta\mathbf{U}^H \tag{28}$$

$$\mathbf{\Omega}_\beta = (\mathbf{J}'_1\mathbf{E}_s)^+(\mathbf{J}'_2\mathbf{E}_s) = \mathbf{U}\mathbf{\Theta}_\beta\mathbf{U}^H \tag{29}$$

From (28) and (29), it can been seen that the requirement of joint diagonalization is satisfied according to Theorem 3 of [23]. By defining a set $\mathbf{\Omega} = \{\mathbf{\Omega}_\theta, \mathbf{\Omega}_\beta\}$, we know that there is a unitary matrix $\mathbf{V}$ that is essentially equivalent to $\mathbf{U}$, which minimizes the following nonnegative function

$$f(\mathbf{\Omega}, \mathbf{V}) = \sum_{i=\theta,\beta} \text{off}(\mathbf{V}^H\mathbf{\Omega}_i\mathbf{V}) \tag{30}$$

where $\text{off}(\mathbf{M}_{n\times n}) = \sum_{1\le i\ne j\le n} |M_{ij}|^2$, and matrix $\mathbf{U}$ is called a joint diagonalizer [23]. Since $\mathbf{U}$ is the eigenvector of both $\mathbf{\Omega}_\theta$ and $\mathbf{\Omega}_\beta$, there is no need for pairing between θ and β since the one-to-one correspondence is preserved on the diagonals between eigenvalue matrices $\mathbf{\Theta}_\theta$ and $\mathbf{\Theta}_\beta$. The same joint diagonalization procedure can be implemented by a series of Givens rotations in [23, 24] to obtain the unitary matrix $\mathbf{U}$. The key idea of joint diagonalization procedure is to achieve simultaneous diagonalization via exploiting the

Jacobi-like algorithm with plane rotations, and the detailed pseudo code of joint diagonalization procedure can be seen in [24].

Then we have eigenvalues of $\mathbf{\Omega}_\theta$ and $\mathbf{\Omega}_\beta$ computed as

$$\eta_{\theta_k} = \mathbf{u}_k^H \mathbf{\Omega}_\theta \mathbf{u}_k \tag{31}$$

$$\eta_{\beta_k} = \mathbf{u}_k^H \mathbf{\Omega}_\beta \mathbf{u}_k \tag{32}$$

where $\mathbf{u}_k$ $(k = 1, \ldots, K')$ is the kth column of $\mathbf{U}$. From (31) and (32), it can be easily obtained that

$$\theta_k = \arccos\left(\frac{\lambda \arg(\eta_{\theta_k})}{2\pi d_x}\right) \tag{33}$$

$$\beta_k = \arccos\left(\frac{\lambda \arg(\eta_{\beta_k})}{2\pi d_y}\right) \tag{34}$$

It should be noted that due to the decomposition of each circular source into two strictly non-circular sources, we have obtained K' angle estimates for either θ_k or β_k, while only K actual 2-D DOAs are present. Thus, we need to correctly pair the two estimates obtained for each circular source in a suitable manner. Actually, this can be easily done by finding the same estimates for each θ_k or β_k and then calculating the average of two identical estimates for 2-D DOA $\theta_{c,k}$ and $\beta_{c,k}(k = 1, \ldots, K_c)$ respectively as

$$\theta_{c,k} = \frac{(\theta_{c,k}^1 + \theta_{c,k}^2)}{2} \tag{35}$$

$$\beta_{c,k} = \frac{(\beta_{c,k}^1 + \beta_{c,k}^2)}{2} \tag{36}$$

Clearly, due to the automatically paired relationship between θ_k and β_k, all the circular sources have been separated provided that either θ_k or β_k is different between any two sources. The proposed method for 2-D DOA

Table 1: Summary of the proposed method.

Input: $\{\hat{\tilde{\mathbf{x}}}(l)\}_{l=1}^{L}$: L snapshots of the new constructed array output vector.
Output: $\hat{\theta}_k$ and $\hat{\beta}_k$: pair-free 2-D estimated angles of K mixed signals.
Step 1 Estimate the covariance matrix $\hat{\mathbf{R}} \approx \frac{1}{L}\sum_{l=1}^{L} \hat{\tilde{\mathbf{x}}}(l)\hat{\tilde{\mathbf{x}}}^H(l)$.
Step 2 Perform subspace decomposition $\hat{\mathbf{R}} = \hat{\mathbf{U}}_s\hat{\mathbf{\Lambda}}_s\hat{\mathbf{U}}_s^H + \hat{\mathbf{U}}_n\hat{\mathbf{\Lambda}}_n\hat{\mathbf{U}}_n^H$ to get $\hat{\mathbf{U}}_s$, and then compute $\hat{\mathbf{E}}_s = \hat{\mathbf{U}}_s\hat{\mathbf{\Lambda}}_s^{\frac{1}{2}}$.
Step 3 Construct two direction matrices $\hat{\mathbf{\Omega}}_\theta = (\mathbf{J}_1\hat{\mathbf{E}}_s)^+(\mathbf{J}_2\hat{\mathbf{E}}_s)$ and $\hat{\mathbf{\Omega}}_\beta = (\mathbf{J}_1'\hat{\mathbf{E}}_s)^+(\mathbf{J}_2'\hat{\mathbf{E}}_s)$.
Step 4 Implement the joint diagonalization to the set $\hat{\mathbf{\Omega}} = \{\hat{\mathbf{\Omega}}_\theta, \hat{\mathbf{\Omega}}_\beta\}$ to obtain the unitary matrix $\hat{\mathbf{U}}$ by a series of Givens rotations.
Step 5 Compute the eigenvalues $\hat{\eta}_{\theta_k} = \hat{\mathbf{u}}_k^H\hat{\mathbf{\Omega}}_\theta\hat{\mathbf{u}}_k$ and $\hat{\eta}_{\beta_k} = \hat{\mathbf{u}}_k^H\hat{\mathbf{\Omega}}_\beta\hat{\mathbf{u}}_k$
Step 6 Compute the 2-D DOAs as $\hat{\theta}_k = \arccos\left(\frac{\lambda \arg(\hat{\eta}_{\theta_k})}{2\pi d_x}\right)$ and $\hat{\beta}_k = \arccos\left(\frac{\lambda \arg(\hat{\eta}_{\beta_k})}{2\pi d_y}\right)$ $(k = 1, \ldots, K')$
Step 7 Compute the 2-D DOAs of circular signals as $\hat{\theta}_{c,k} = \frac{(\hat{\theta}_{c,k}^1 + \hat{\theta}_{c,k}^2)}{2}$ and $\hat{\beta}_{c,k} = \frac{(\hat{\beta}_{c,k}^1 + \hat{\beta}_{c,k}^2)}{2}$ $(k = 1, \ldots, K_c)$

estimation under the mixed circular and strictly noncircular sources is summarized in Table 1.

Remark 2: Since the noncircularity information is used in the proposed method, the equivalent number of degrees of freedom of the array is increased compared to the method in [21]. The maximum number of identifiable targets by the proposed method is $K_n + 2K_c = min\{2M(N-1), 2N(M-1)\}$, while that of the method in [21] must satisfy $K_n + K_c = min\{M(N-1), N(M-1)\}$. Therefore, our method can distinguish more signals than the method in [21], when at least two strictly non-circular sources are present in the mixed signals.

Remark 3: The major part of the computational effort of the proposed method includes the construction of $\hat{\mathbf{R}}$, performing EVD of $\hat{\mathbf{R}}$, and joint diagonalization of the set $\mathbf{\Omega}$. To calculate $\hat{\mathbf{R}}$, we need $O\left((2MN)^2 L\right)$ complex multiplications; the EVD operation of $\hat{\mathbf{R}}$ requires the amount of complex multiplications of $O\left((2MN)^3\right)$; and jointly diagonalizing the set $\mathbf{\Omega}$ (two $K' \times K'$ direction matrices), is of $O\left(2(K')^3\right)$. Then, the total computational complexity of the proposed method in terms of complex multiplications is about $O\left((2MN)^2 L + (2MN)^3 + 2(K')^3\right)$.

Remark 4: The proposed method is also applicable to the case where all the incoming signals are noncircular signals (Case 4) since the uniqueness of joint diagonalization is still satisfied for this case. The simulation results in section IV will demonstrate the correctness of Case 4. And the 2-D angle estimation of Case 4 is more accurate than that of the mixed cases.

4. Theoretical error performance analysis

In this section, the theoretical error performance analysis of the proposed method is conducted. The derivation in this paper is along the lines of the first-order analysis done by Rao [25] and the backward error analysis by Li [26]. To analyze the proposed subspace algorithm, it is important to analyze the subspace perturbation. First, subspace decomposition can also be performed using singular value decomposition (SVD) of $\tilde{\mathbf{x}}$ as follows:

$$\tilde{\mathbf{x}} = \begin{pmatrix} \mathbf{U}_s & \mathbf{U}_n \end{pmatrix} \begin{pmatrix} \mathbf{\Sigma}_s & \mathbf{0} \\ \mathbf{0} & \mathbf{0} \end{pmatrix} \begin{pmatrix} \mathbf{V}_s^H \\ \mathbf{V}_n^H \end{pmatrix} \tag{37}$$

Following the first-order approximation principles [25, 26] for eigenvalues in (31) and (32), we have

$$\delta\eta_{\theta_k} \approx \mathbf{u}_k^H \delta\mathbf{\Omega}_\theta \mathbf{u}_k = \mathbf{u}_k^H (\mathbf{J}_1\mathbf{U}_x)^+ (\delta\mathbf{U}_{x2} - \delta\mathbf{U}_{x1}\mathbf{\Omega}_\theta)\,\mathbf{u}_k \tag{38}$$

$$\delta\eta_{\beta_k} \approx \mathbf{u}_k^H \delta\mathbf{\Omega}_\beta \mathbf{u}_k = \mathbf{u}_k^H (\mathbf{J}_1'\mathbf{U}_x)^+ (\delta\mathbf{U}_{x2} - \delta\mathbf{U}_{x1}\mathbf{\Omega}_\beta)\,\mathbf{u}_k \tag{39}$$

where

$$\mathbf{U}_x = \mathbf{U}_s\mathbf{\Sigma}_\mathbf{s} \tag{40}$$

$$\delta\mathbf{U}_x = \delta\mathbf{U}_s\mathbf{\Sigma}_\mathbf{s} \tag{41}$$

$$\delta\mathbf{U}_s = \mathbf{U}_n\mathbf{U}_n^H\breve{\mathbf{n}}\mathbf{V}_s\mathbf{\Sigma}_\mathbf{s}^{-\mathbf{1}} \tag{42}$$

According to (41) and (42), we obtain

$$\delta\mathbf{U}_{x1} = \mathbf{J}_1\delta\mathbf{U}_x = (\mathbf{J}_1\mathbf{U}_n)\,\mathbf{U}_n^H\breve{\mathbf{n}}\mathbf{V}_s \tag{43}$$

$$\delta\mathbf{U}_{x2} = \mathbf{J}_2\delta\mathbf{U}_x = (\mathbf{J}_2\mathbf{U}_n)\,\mathbf{U}_n^H\breve{\mathbf{n}}\mathbf{V}_s \tag{44}$$

$$\delta\mathbf{U}_{x1}' = \mathbf{J}_1'\delta\mathbf{U}_x = (\mathbf{J}_1'\mathbf{U}_n)\,\mathbf{U}_n^H\breve{\mathbf{n}}\mathbf{V}_s \tag{45}$$

$$\delta \mathbf{U}'_{x2} = \mathbf{J}'_2 \delta \mathbf{U}_x = \left(\mathbf{J}'_2 \mathbf{U}_n\right) \mathbf{U}_n^H \breve{\mathbf{n}} \mathbf{V}_s \tag{46}$$

Then, by substituting (43) and (44) into (38), (45) and (46) into (39), (38) and (39) can be rewritten as

$$\delta \eta_{\theta_k} \approx \mathbf{u}_k^H \left(\mathbf{J}_1 \mathbf{U}_x\right)^+ \left(\mathbf{J}_2 \mathbf{U}_n - \eta_{\theta_k} \mathbf{J}_1 \mathbf{U}_n\right) \mathbf{U}_n^H \breve{\mathbf{n}} \mathbf{V}_s \mathbf{u}_k \tag{47}$$

$$\delta \eta_{\beta_k} \approx \mathbf{u}_k^H \left(\mathbf{J}'_1 \mathbf{U}_x\right)^+ \left(\mathbf{J}'_2 \mathbf{U}_n - \eta_{\beta_k} \mathbf{J}'_1 \mathbf{U}_n\right) \mathbf{U}_n^H \breve{\mathbf{n}} \mathbf{V}_s \mathbf{u}_k \tag{48}$$

Using the first-order Taylor series expansion [25, 26], the perturbation of the kth ($k = 1, \ldots, K'$) θ and β can be expressed as

$$\delta \theta_k = \nu_{\theta_k} \mathrm{Im}\left(\frac{\delta \eta_{\theta_k}}{\eta_{\theta_k}}\right) \tag{49}$$

$$\delta \beta_k = \nu_{\beta_k} \mathrm{Im}\left(\frac{\delta \eta_{\beta_k}}{\eta_{\beta_k}}\right) \tag{50}$$

where $\nu_{\theta_k}{=}\lambda/(2\pi d_x \sin\theta_k)$ and $\nu_{\beta_k}{=}\lambda/(2\pi d_y \sin\beta_k)$. The error-variance of the estimated 2-D DOAs are

$$\mathrm{var}\left(\delta\theta_k\right) = \frac{1}{2}\nu_{\theta_k}^2 \mathrm{var}\left(\frac{\boldsymbol{\xi}_{\theta_k}^H \breve{\mathbf{n}} \boldsymbol{\vartheta}_k}{\eta_{\theta_k}}\right) = \frac{\nu_{\theta_k}^2 \sigma^2}{2} \frac{\boldsymbol{\xi}_{\theta_k}^H \boldsymbol{\xi}_{\theta_k} \boldsymbol{\vartheta}_k^H \boldsymbol{\vartheta}_k}{\left|\eta_{\theta_k}\right|^2} \tag{51}$$

$$\mathrm{var}\left(\delta\beta_k\right) = \frac{1}{2}\nu_{\beta_k}^2 \mathrm{var}\left(\frac{\boldsymbol{\xi}_{\beta_k}^H \breve{\mathbf{n}} \boldsymbol{\vartheta}_k}{\eta_{\beta_k}}\right) = \frac{\nu_{\beta_k}^2 \sigma^2}{2} \frac{\boldsymbol{\xi}_{\beta_k}^H \boldsymbol{\xi}_{\beta_k} \boldsymbol{\vartheta}_k^H \boldsymbol{\vartheta}_k}{\left|\eta_{\beta_k}\right|^2} \tag{52}$$

where

$$\boldsymbol{\xi}_{\theta_k}^H = \mathbf{u}_k^H \left(\mathbf{J}_1 \mathbf{U}_x\right)^+ \left(\mathbf{J}_2 \mathbf{U}_n - \eta_{\theta_k} \mathbf{J}_1 \mathbf{U}_n\right) \mathbf{U}_n^H \tag{53}$$

$$\boldsymbol{\xi}_{\beta_k}^H = \mathbf{u}_k^H \left(\mathbf{J}'_1 \mathbf{U}_x\right)^+ \left(\mathbf{J}'_2 \mathbf{U}_n - \eta_{\beta_k} \mathbf{J}'_1 \mathbf{U}_n\right) \mathbf{U}_n^H \tag{54}$$

$$\boldsymbol{\vartheta}_k = \mathbf{V}_s \mathbf{u}_k \tag{55}$$

$$\left|\eta_{\theta_k}\right| = \left|\eta_{\beta_k}\right| = 1 \tag{56}$$

For the kth ($k = 1, \ldots, K_c$) circular signals, the variances of the two estimated angles are given by

$$\mathrm{var}\left(\delta\theta_{c,k}\right) = \left[\mathrm{var}\left(\delta\theta_{c,k}^{1}\right) + \mathrm{var}\left(\delta\theta_{c,k}^{2}\right)\right]/2 \tag{57}$$

$$\mathrm{var}\left(\delta\beta_{c,k}\right) = \left[\mathrm{var}\left(\delta\beta_{c,k}^{1}\right) + \mathrm{var}\left(\delta\beta_{c,k}^{2}\right)\right]/2 \tag{58}$$

5. Cramer-Rao bound (CRB) analysis

In this section, we derive the closed-form expression of the deterministic CRB of 2-D DOAs for the mixed signals scenario. With (8), the model in (1) can be rewritten as

$$\mathbf{x} = \mathbf{A}_n \mathbf{\Psi} \mathbf{s}_n + \mathbf{A}_c \mathbf{s}_c + \mathbf{n} \tag{59}$$

The desired CRB matrix is usually computed by taking the inverse of the Fisher information matrix (FIM) $\mathbf{F}$ for the interest parameter $\boldsymbol{\theta} = [\theta_{n,1}, \theta_{n,2}, \ldots, \theta_{n,K_n}, \theta_{c,1}, \theta_{c,2}, \ldots, \theta_{c,K_c}]$ and $\boldsymbol{\beta} = [\beta_{n,1}, \beta_{n,2}, \ldots, \beta_{n,K_n}, \beta_{c,1}, \beta_{c,2}, \ldots, \beta_{c,K_c}]$. $\mathbf{F}$ can be written as

$$\mathbf{F} = \begin{bmatrix} \mathbf{F}_{\boldsymbol{\theta}_n\boldsymbol{\theta}_n} & \mathbf{F}_{\boldsymbol{\theta}_n\boldsymbol{\theta}_c} & \mathbf{F}_{\boldsymbol{\theta}_n\boldsymbol{\beta}_n} & \mathbf{F}_{\boldsymbol{\theta}_n\boldsymbol{\beta}_c} \\ \mathbf{F}_{\boldsymbol{\theta}_c\boldsymbol{\theta}_n} & \mathbf{F}_{\boldsymbol{\theta}_c\boldsymbol{\theta}_c} & \mathbf{F}_{\boldsymbol{\theta}_c\boldsymbol{\beta}_n} & \mathbf{F}_{\boldsymbol{\theta}_c\boldsymbol{\beta}_c} \\ \mathbf{F}_{\boldsymbol{\beta}_n\boldsymbol{\theta}_n} & \mathbf{F}_{\boldsymbol{\beta}_n\boldsymbol{\theta}_c} & \mathbf{F}_{\boldsymbol{\beta}_n\boldsymbol{\beta}_n} & \mathbf{F}_{\boldsymbol{\beta}_n\boldsymbol{\beta}_c} \\ \mathbf{F}_{\boldsymbol{\beta}_c\boldsymbol{\theta}_n} & \mathbf{F}_{\boldsymbol{\beta}_c\boldsymbol{\theta}_c} & \mathbf{F}_{\boldsymbol{\beta}_c\boldsymbol{\beta}_n} & \mathbf{F}_{\boldsymbol{\beta}_c\boldsymbol{\beta}_c} \end{bmatrix} \tag{60}$$

Note that the (i,j)th element of $\mathbf{F}_{\boldsymbol{\theta}_n\boldsymbol{\theta}_n}$ [27, 28] is given by

$$\begin{aligned} \mathbf{F}(\theta_{n,i}, \theta_{n,j}) &= 2\,\mathrm{Re}\{tr[(\dot{\mathbf{A}}_{\theta_{n,i}}\mathbf{\Psi}\mathbf{s}_n)^H \boldsymbol{\gamma}^{-1}(\dot{\mathbf{A}}_{\theta_{n,j}}\mathbf{\Psi}\mathbf{s}_n)]\} \\ &= 2\,\mathrm{Re}\{tr[(\dot{\mathbf{A}}_{\theta_n}\mathbf{\Psi}\mathbf{e}_i\mathbf{e}_i^T\mathbf{s}_n)^H \boldsymbol{\gamma}^{-1}(\dot{\mathbf{A}}_{\theta_n}\mathbf{\Psi}\mathbf{e}_j\mathbf{e}_j^T\mathbf{s}_n)]\} \\ &= 2\,\mathrm{Re}[(\mathbf{e}_i^T\mathbf{\Psi}^H\dot{\mathbf{A}}_{\theta_n}^H\boldsymbol{\gamma}^{-1}\dot{\mathbf{A}}_{\theta_n}\mathbf{\Psi}\mathbf{e}_j)(\mathbf{e}_j^T\mathbf{s}_n\mathbf{s}_n^H\mathbf{e}_i)] \\ &= 2L\,\mathrm{Re}[(\mathbf{\Psi}^H\dot{\mathbf{A}}_{\theta_n}^H\boldsymbol{\gamma}^{-1}\dot{\mathbf{A}}_{\theta_n}\mathbf{\Psi})_{ij}(\mathbf{R}_{s_ns_n}^T)_{ij}] \end{aligned} \tag{61}$$

Due to $\mathbf{F}=\mathbf{F}^T$, we only need to calculate the upper triangular block matrices of $\mathbf{F}$. Similarly, we get the (i,j)th element of block matrix $\mathbf{F}_{\boldsymbol{\theta}_n\boldsymbol{\theta}_c}$, $\mathbf{F}_{\boldsymbol{\theta}_n\boldsymbol{\beta}_n}$, $\mathbf{F}_{\boldsymbol{\theta}_n\boldsymbol{\beta}_c}$, $\mathbf{F}_{\boldsymbol{\theta}_c\boldsymbol{\theta}_c}$, $\mathbf{F}_{\boldsymbol{\theta}_c\boldsymbol{\beta}_n}$, $\mathbf{F}_{\boldsymbol{\theta}_c\boldsymbol{\beta}_c}$, $\mathbf{F}_{\boldsymbol{\beta}_n\boldsymbol{\beta}_n}$, $\mathbf{F}_{\boldsymbol{\beta}_n\boldsymbol{\beta}_c}$ and $\mathbf{F}_{\boldsymbol{\beta}_c\boldsymbol{\beta}_c}$ respectively, as follows

$$\begin{aligned}\mathbf{F}(\theta_{n,i},\theta_{c,j}) &= 2\,\mathrm{Re}\{tr[(\dot{\mathbf{A}}_{\theta_{n,i}}\boldsymbol{\Psi}\mathbf{s}_n)^H\boldsymbol{\gamma}^{-1}(\dot{\mathbf{A}}_{\theta_{c,j}}\mathbf{s}_c)]\}\\ &= 2\,\mathrm{Re}\{tr[(\dot{\mathbf{A}}_{\theta_n}\boldsymbol{\Psi}\mathbf{e}_i\mathbf{e}_i^T\mathbf{s}_n)^H\boldsymbol{\gamma}^{-1}(\dot{\mathbf{A}}_{\theta_c}\mathbf{e}_j\mathbf{e}_j^T\mathbf{s}_c)]\}\\ &= 2\,\mathrm{Re}[(\mathbf{e}_i^T\boldsymbol{\Psi}^H\dot{\mathbf{A}}_{\theta_n}^H\boldsymbol{\gamma}^{-1}\dot{\mathbf{A}}_{\theta_c}\mathbf{e}_j)(\mathbf{e}_j^T\mathbf{s}_c\mathbf{s}_n^H\mathbf{e}_i)]\\ &= 2L\,\mathrm{Re}[(\boldsymbol{\Psi}^H\dot{\mathbf{A}}_{\theta_n}^H\boldsymbol{\gamma}^{-1}\dot{\mathbf{A}}_{\theta_c})_{ij}(\mathbf{R}_{s_cs_n}^T)_{ij}]\end{aligned} \tag{62}$$

$$\begin{aligned}\mathbf{F}(\theta_{n,i},\beta_{n,j}) &= 2\,\mathrm{Re}\{tr[(\dot{\mathbf{A}}_{\theta_{n,i}}\boldsymbol{\Psi}\mathbf{s}_n)^H\boldsymbol{\gamma}^{-1}(\dot{\mathbf{A}}_{\beta_{n,j}}\boldsymbol{\Psi}\mathbf{s}_n)]\}\\ &= 2\,\mathrm{Re}\{tr[(\dot{\mathbf{A}}_{\theta_n}\boldsymbol{\Psi}\mathbf{e}_i\mathbf{e}_i^T\mathbf{s}_n)^H\boldsymbol{\gamma}^{-1}(\dot{\mathbf{A}}_{\beta_n}\boldsymbol{\Psi}\mathbf{e}_j\mathbf{e}_j^T\mathbf{s}_n)]\}\\ &= 2\,\mathrm{Re}[(\mathbf{e}_i^T\boldsymbol{\Psi}^H\dot{\mathbf{A}}_{\theta_n}^H\boldsymbol{\gamma}^{-1}\dot{\mathbf{A}}_{\beta_n}\boldsymbol{\Psi}\mathbf{e}_j)(\mathbf{e}_j^T\mathbf{s}_n\mathbf{s}_n^H\mathbf{e}_i)]\\ &= 2L\,\mathrm{Re}[(\boldsymbol{\Psi}^H\dot{\mathbf{A}}_{\theta_n}^H\boldsymbol{\gamma}^{-1}\dot{\mathbf{A}}_{\beta_n}\boldsymbol{\Psi})_{ij}(\mathbf{R}_{s_ns_n}^T)_{ij}]\end{aligned} \tag{63}$$

$$\begin{aligned}\mathbf{F}(\theta_{n,i},\beta_{c,j}) &= 2\,\mathrm{Re}\{tr[(\dot{\mathbf{A}}_{\theta_{n,i}}\boldsymbol{\Psi}\mathbf{s}_n)^H\boldsymbol{\gamma}^{-1}(\dot{\mathbf{A}}_{\beta_{c,j}}\mathbf{s}_c)]\}\\ &= 2\,\mathrm{Re}\{tr[(\dot{\mathbf{A}}_{\theta_n}\boldsymbol{\Psi}\mathbf{e}_i\mathbf{e}_i^T\mathbf{s}_n)^H\boldsymbol{\gamma}^{-1}(\dot{\mathbf{A}}_{\beta_c}\mathbf{e}_j\mathbf{e}_j^T\mathbf{s}_c)]\}\\ &= 2\,\mathrm{Re}[(\mathbf{e}_i^T\boldsymbol{\Psi}^H\dot{\mathbf{A}}_{\theta_n}^H\boldsymbol{\gamma}^{-1}\dot{\mathbf{A}}_{\beta_c}\mathbf{e}_j)(\mathbf{e}_j^T\mathbf{s}_c\mathbf{s}_n^H\mathbf{e}_i)]\\ &= 2L\,\mathrm{Re}[(\boldsymbol{\Psi}^H\dot{\mathbf{A}}_{\theta_n}^H\boldsymbol{\gamma}^{-1}\dot{\mathbf{A}}_{\beta_c})_{ij}(\mathbf{R}_{s_cs_n}^T)_{ij}]\end{aligned} \tag{64}$$

$$\begin{aligned}\mathbf{F}(\theta_{c,i},\theta_{c,j}) &= 2\,\mathrm{Re}\{tr[(\dot{\mathbf{A}}_{\theta_{c,i}}\mathbf{s}_c)^H\boldsymbol{\gamma}^{-1}(\dot{\mathbf{A}}_{\theta_{c,j}}\mathbf{s}_c)]\}\\ &= 2\,\mathrm{Re}\{tr[(\dot{\mathbf{A}}_{\theta_c}\mathbf{e}_i\mathbf{e}_i^T\mathbf{s}_c)^H\boldsymbol{\gamma}^{-1}(\dot{\mathbf{A}}_{\theta_c}\mathbf{e}_j\mathbf{e}_j^T\mathbf{s}_c)]\}\\ &= 2\,\mathrm{Re}[(\mathbf{e}_i^T\dot{\mathbf{A}}_{\theta_c}^H\boldsymbol{\gamma}^{-1}\dot{\mathbf{A}}_{\theta_c}\mathbf{e}_j)(\mathbf{e}_j^T\mathbf{s}_c\mathbf{s}_c^H\mathbf{e}_i)]\\ &= 2L\,\mathrm{Re}[(\dot{\mathbf{A}}_{\theta_c}^H\boldsymbol{\gamma}^{-1}\dot{\mathbf{A}}_{\theta_c})_{ij}(\mathbf{R}_{s_cs_c}^T)_{ij}]\end{aligned} \tag{65}$$

$$
\begin{aligned}
\mathbf{F}(\theta_{c,i},\beta_{n,j}) &= 2\,\mathrm{Re}\{tr[(\dot{\mathbf{A}}_{\theta_{c,i}}\mathbf{s}_c)^H\boldsymbol{\gamma}^{-1}(\dot{\mathbf{A}}_{\beta_{n,j}}\boldsymbol{\Psi}\mathbf{s}_n)]\}\\
&= 2\,\mathrm{Re}\{tr[(\dot{\mathbf{A}}_{\theta_c}\mathbf{e}_i\mathbf{e}_i^T\mathbf{s}_c)^H\boldsymbol{\gamma}^{-1}(\dot{\mathbf{A}}_{\beta_n}\boldsymbol{\Psi}\mathbf{e}_j\mathbf{e}_j^T\mathbf{s}_n)]\}\\
&= 2\,\mathrm{Re}[(\mathbf{e}_i^T\dot{\mathbf{A}}_{\theta_c}^H\boldsymbol{\gamma}^{-1}\dot{\mathbf{A}}_{\beta_n}\boldsymbol{\Psi}\mathbf{e}_j)(\mathbf{e}_j^T\mathbf{s}_n\mathbf{s}_c^H\mathbf{e}_i)]\\
&= 2L\,\mathrm{Re}[(\dot{\mathbf{A}}_{\theta_c}^H\boldsymbol{\gamma}^{-1}\dot{\mathbf{A}}_{\beta_n}\boldsymbol{\Psi})_{ij}(\mathbf{R}_{s_ns_c}^T)_{ij}]
\end{aligned}
\tag{66}
$$

$$
\begin{aligned}
\mathbf{F}(\theta_{c,i},\beta_{c,j}) &= 2\,\mathrm{Re}\{tr[(\dot{\mathbf{A}}_{\theta_{c,i}}\mathbf{s}_c)^H\boldsymbol{\gamma}^{-1}(\dot{\mathbf{A}}_{\beta_{c,j}}\mathbf{s}_c)]\}\\
&= 2\,\mathrm{Re}\{tr[(\dot{\mathbf{A}}_{\theta_c}\mathbf{e}_i\mathbf{e}_i^T\mathbf{s}_c)^H\boldsymbol{\gamma}^{-1}(\dot{\mathbf{A}}_{\beta_c}\mathbf{e}_j\mathbf{e}_j^T\mathbf{s}_c)]\}\\
&= 2\,\mathrm{Re}[(\mathbf{e}_i^T\dot{\mathbf{A}}_{\theta_c}^H\boldsymbol{\gamma}^{-1}\dot{\mathbf{A}}_{\beta_c}\mathbf{e}_j)(\mathbf{e}_j^T\mathbf{s}_c\mathbf{s}_c^H\mathbf{e}_i)]\\
&= 2L\,\mathrm{Re}[(\dot{\mathbf{A}}_{\theta_c}^H\boldsymbol{\gamma}^{-1}\dot{\mathbf{A}}_{\beta_c})_{ij}(\mathbf{R}_{s_cs_c}^T)_{ij}]
\end{aligned}
\tag{67}
$$

$$
\begin{aligned}
\mathbf{F}(\beta_{n,i},\beta_{n,j}) &= 2\,\mathrm{Re}\{tr[(\dot{\mathbf{A}}_{\beta_{n,i}}\boldsymbol{\Psi}\mathbf{s}_n)^H\boldsymbol{\gamma}^{-1}(\dot{\mathbf{A}}_{\beta_{n,j}}\boldsymbol{\Psi}\mathbf{s}_n)]\}\\
&= 2\,\mathrm{Re}\{tr[(\dot{\mathbf{A}}_{\beta_n}\boldsymbol{\Psi}\mathbf{e}_i\mathbf{e}_i^T\mathbf{s}_n)^H\boldsymbol{\gamma}^{-1}(\dot{\mathbf{A}}_{\beta_n}\boldsymbol{\Psi}\mathbf{e}_j\mathbf{e}_j^T\mathbf{s}_n)]\}\\
&= 2\,\mathrm{Re}[(\mathbf{e}_i^T\boldsymbol{\Psi}^H\dot{\mathbf{A}}_{\beta_n}^H\boldsymbol{\gamma}^{-1}\dot{\mathbf{A}}_{\beta_n}\boldsymbol{\Psi}\mathbf{e}_j)(\mathbf{e}_j^T\mathbf{s}_n\mathbf{s}_n^H\mathbf{e}_i)]\\
&= 2L\,\mathrm{Re}[(\boldsymbol{\Psi}^H\dot{\mathbf{A}}_{\beta_n}^H\boldsymbol{\gamma}^{-1}\dot{\mathbf{A}}_{\beta_n}\boldsymbol{\Psi})_{ij}(\mathbf{R}_{s_ns_n}^T)_{ij}]
\end{aligned}
\tag{68}
$$

$$
\begin{aligned}
\mathbf{F}(\beta_{n,i},\beta_{c,j}) &= 2\,\mathrm{Re}\{tr[(\dot{\mathbf{A}}_{\beta_{n,i}}\boldsymbol{\Psi}\mathbf{s}_n)^H\boldsymbol{\gamma}^{-1}(\dot{\mathbf{A}}_{\beta_{c,j}}\mathbf{s}_c)]\}\\
&= 2\,\mathrm{Re}\{tr[(\dot{\mathbf{A}}_{\beta_n}\boldsymbol{\Psi}\mathbf{e}_i\mathbf{e}_i^T\mathbf{s}_n)^H\boldsymbol{\gamma}^{-1}(\dot{\mathbf{A}}_{\beta_c}\mathbf{e}_j\mathbf{e}_j^T\mathbf{s}_c)]\}\\
&= 2\,\mathrm{Re}[(\mathbf{e}_i^T\boldsymbol{\Psi}^H\dot{\mathbf{A}}_{\beta_n}^H\boldsymbol{\gamma}^{-1}\dot{\mathbf{A}}_{\beta_c}\mathbf{e}_j)(\mathbf{e}_j^T\mathbf{s}_c\mathbf{s}_n^H\mathbf{e}_i)]\\
&= 2L\,\mathrm{Re}[(\boldsymbol{\Psi}^H\dot{\mathbf{A}}_{\beta_n}^H\boldsymbol{\gamma}^{-1}\dot{\mathbf{A}}_{\beta_c})_{ij}(\mathbf{R}_{s_cs_n}^T)_{ij}]
\end{aligned}
\tag{69}
$$

$$
\begin{aligned}
\mathbf{F}(\beta_{c,i},\beta_{c,j}) &= 2\,\mathrm{Re}\{tr[(\dot{\mathbf{A}}_{\beta_{c,i}}\mathbf{s}_c)^H\boldsymbol{\gamma}^{-1}(\dot{\mathbf{A}}_{\beta_{c,j}}\mathbf{s}_c)]\}\\
&= 2\,\mathrm{Re}\{tr[(\dot{\mathbf{A}}_{\beta_c}\mathbf{e}_i\mathbf{e}_i^T\mathbf{s}_c)^H\boldsymbol{\gamma}^{-1}(\dot{\mathbf{A}}_{\beta_c}\mathbf{e}_j\mathbf{e}_j^T\mathbf{s}_c)]\}\\
&= 2\,\mathrm{Re}[(\mathbf{e}_i^T\dot{\mathbf{A}}_{\beta_c}^H\boldsymbol{\gamma}^{-1}\dot{\mathbf{A}}_{\beta_c}\mathbf{e}_j)(\mathbf{e}_j^T\mathbf{s}_c\mathbf{s}_c^H\mathbf{e}_i)]\\
&= 2L\,\mathrm{Re}[(\dot{\mathbf{A}}_{\beta_c}^H\boldsymbol{\gamma}^{-1}\dot{\mathbf{A}}_{\beta_c})_{ij}(\mathbf{R}_{s_cs_c}^T)_{ij}]
\end{aligned}
\tag{70}
$$

where $\dot{\mathbf{A}}_{\varsigma_n}$, $\dot{\mathbf{A}}_{\varsigma_c}$ $(\varsigma = \theta, \beta)$, $\mathbf{R}_{s_n s_n}$, $\mathbf{R}_{s_n s_c}$, $\mathbf{R}_{s_c s_n}$ and $\mathbf{R}_{s_c s_c}$ has the form of

$$\dot{\mathbf{A}}_{\varsigma_n} = \left[\frac{\partial \mathbf{A}}{\partial \varsigma_1}, \frac{\partial \mathbf{A}}{\partial \varsigma_2}, ..., \frac{\partial \mathbf{A}}{\partial \varsigma_{K_n}}\right] \tag{71}$$

$$\dot{\mathbf{A}}_{\varsigma_c} = \left[\frac{\partial \mathbf{A}}{\partial \varsigma_1}, \frac{\partial \mathbf{A}}{\partial \varsigma_2}, ..., \frac{\partial \mathbf{A}}{\partial \varsigma_{K_c}}\right] \tag{72}$$

$$\mathbf{R}_{s_n s_n} = \frac{1}{L} \mathbf{s}_n \mathbf{s}_n^H \tag{73}$$

$$\mathbf{R}_{s_n s_c} = \frac{1}{L} \mathbf{s}_n \mathbf{s}_c^H \tag{74}$$

$$\mathbf{R}_{s_c s_n} = \frac{1}{L} \mathbf{s}_c \mathbf{s}_n^H \tag{75}$$

$$\mathbf{R}_{s_c s_c} = \frac{1}{L} \mathbf{s}_c \mathbf{s}_c^H \tag{76}$$

for white noise, $\boldsymbol{\gamma}$ has the form of $\sigma^2 \mathbf{I}_{MN}$.

According to equations from (71) to (76), we obtain

$$\mathbf{F}_{\boldsymbol{\theta}_n \boldsymbol{\theta}_n} = 2L \,\mathrm{Re}[(\boldsymbol{\Psi}^H \dot{\mathbf{A}}_{\theta_n}^H \boldsymbol{\gamma}^{-1} \dot{\mathbf{A}}_{\theta_n} \boldsymbol{\Psi}) \otimes (\mathbf{R}_{s_n s_n}^T)] \tag{77}$$

$$\mathbf{F}_{\boldsymbol{\theta}_n \boldsymbol{\theta}_c} = 2L \,\mathrm{Re}[(\boldsymbol{\Psi}^H \dot{\mathbf{A}}_{\theta_n}^H \boldsymbol{\gamma}^{-1} \dot{\mathbf{A}}_{\theta_c}) \otimes (\mathbf{R}_{s_c s_n}^T)] \tag{78}$$

$$\mathbf{F}_{\boldsymbol{\theta}_n \boldsymbol{\beta}_n} = 2L \,\mathrm{Re}[(\boldsymbol{\Psi}^H \dot{\mathbf{A}}_{\theta_n}^H \boldsymbol{\gamma}^{-1} \dot{\mathbf{A}}_{\beta_n} \boldsymbol{\Psi}) \otimes (\mathbf{R}_{s_n s_n}^T)] \tag{79}$$

$$\mathbf{F}_{\boldsymbol{\theta}_n \boldsymbol{\beta}_c} = 2L \,\mathrm{Re}[(\boldsymbol{\Psi}^H \dot{\mathbf{A}}_{\theta_n}^H \boldsymbol{\gamma}^{-1} \dot{\mathbf{A}}_{\beta_c}) \otimes (\mathbf{R}_{s_c s_n}^T)] \tag{80}$$

$$\mathbf{F}_{\boldsymbol{\theta}_c \boldsymbol{\theta}_c} = 2L \,\mathrm{Re}[(\dot{\mathbf{A}}_{\theta_c}^H \boldsymbol{\gamma}^{-1} \dot{\mathbf{A}}_{\theta_c}) \otimes (\mathbf{R}_{s_c s_c}^T)] \tag{81}$$

$$\mathbf{F}_{\boldsymbol{\theta}_c \boldsymbol{\beta}_n} = 2L \,\mathrm{Re}[(\dot{\mathbf{A}}_{\theta_c}^H \boldsymbol{\gamma}^{-1} \dot{\mathbf{A}}_{\beta_n} \boldsymbol{\Psi}) \otimes (\mathbf{R}_{s_n s_c}^T)] \tag{82}$$

$$\mathbf{F}_{\boldsymbol{\theta}_c \boldsymbol{\beta}_c} = 2L \,\mathrm{Re}[(\dot{\mathbf{A}}_{\theta_c}^H \boldsymbol{\gamma}^{-1} \dot{\mathbf{A}}_{\beta_c}) \otimes (\mathbf{R}_{s_c s_c}^T)] \tag{83}$$

$$\mathbf{F}_{\boldsymbol{\beta}_n \boldsymbol{\beta}_n} = 2L \,\mathrm{Re}[(\boldsymbol{\Psi}^H \dot{\mathbf{A}}_{\beta_n}^H \boldsymbol{\gamma}^{-1} \dot{\mathbf{A}}_{\beta_n} \boldsymbol{\Psi}) \otimes (\mathbf{R}_{s_n s_n}^T)] \tag{84}$$

$$\mathbf{F}_{\boldsymbol{\beta}_n \boldsymbol{\beta}_c} = 2L \,\mathrm{Re}[(\boldsymbol{\Psi}^H \dot{\mathbf{A}}_{\beta_n}^H \boldsymbol{\gamma}^{-1} \dot{\mathbf{A}}_{\beta_c}) \otimes (\mathbf{R}_{s_c s_n}^T)] \tag{85}$$

$$\mathbf{F}_{\boldsymbol{\beta}_c \boldsymbol{\beta}_c} = 2L \,\mathrm{Re}[(\dot{\mathbf{A}}_{\beta_c}^H \boldsymbol{\gamma}^{-1} \dot{\mathbf{A}}_{\beta_c}) \otimes (\mathbf{R}_{s_c s_c}^T)] \tag{86}$$

Then the CRB matrix $\mathbf{C}$ can be expressed as

$$\mathbf{C} = \mathbf{F}^{-1} \tag{87}$$

and the individual CRBs of θ and β for the circular signals as well as the strictly non-circular signals can easily be extracted from (87) as follows

$$\mathrm{CRB}_{\theta_i} = \mathbf{C}_{i,i} \tag{88}$$

$$\mathrm{CRB}_{\beta_i} = \mathbf{C}_{i+K,i+K} \tag{89}$$

where $\mathbf{C}_{i,i}$ $(i = 1, 2, \ldots, K)$ denotes the (i,i)th element of $\mathbf{C}$.

It should be pointed out that the above CRB analysis is also applicable to the case where all the incoming signals are noncircular or circular signals.

6. Simulation results

In this section, five sets of simulations are performed to demonstrate the performance of the proposed method. The first set of simulation is based on a URA with $M = 3$ rows and $N = 4$ columns, while for the next three, $N = M = 5$; and for the last one, the number of antennas varies. Both d_x and d_y are half wavelength.

The mixed circular and strictly noncircular signals have an equal power. The power of additive white Gaussian noise is σ_n^2. The signal-to-noise ratio is defined as $\mathrm{SNR} = 10\log_{10}(\sigma_s^2/\sigma_n^2)$. The root mean squared error (RMSE) as defined by $\mathrm{RMSE} = \sqrt{\frac{1}{KM_c}\sum_{k=1}^{K}\sum_{q=1}^{M_c}\left(\hat{\zeta}_{qk} - \zeta_k\right)^2}$ is adopted for quantitative evaluation, where M_c is the number of Monte Carlo simulations, K is the number of signals, $\hat{\zeta}_{q,k}$ is the estimate of the parameter ($\hat{\theta}_k$ or $\hat{\beta}_k$) in the kth Monte Carlo simulation, and ζ_k is the true value standing for either θ_k or

β_k. For comparison, the DOA estimation results obtained using the method in [21], which does not exploit the noncircular information of the signals, the theoretical error performance and CRB of the proposed method are also provided. Note that we cannot compare with the method in [22], because when the angle ambiguity problem emerges, the method in [22] fails to work.

6.1. 2-D DOA estimation

We consider four uncorrelated mixed BPSK and QPSK signals from directions $(60°, 80°)$, $(85°, 70°)$, $(85°, 95°)$ and $(110°, 95°)$, respectively. Four cases are studied corresponding to one, two and four BPSK signals. The SNR is set at 10dB. The number of snapshots is 500, and M_c is 500. Fig.2 (a) to (d) displays the 2-D DOA scattergram of the circular and strictly noncircular signals by both the proposed method and the method in [21], with number of strictly noncircular signals increasing from one to four. It can be seen that the proposed method outperforms the method in [21], especially when the number of strictly noncircular signals increases. This is because the noncircularity information is utilized in the proposed method which increases the effective array aperture.

6.2. Performance versus SNR

In this simulation, we study the performance with respect to a varying SNR ranging from -5dB to 20dB. Here we suppose four uncorrelated mixed signals are from directions $(60°, 50°)$, $(70°, 50°)$, $(70°, 60°)$ and $(80°, 70°)$. Three cases are considered as before starting from $K_n = 1$ associated with $(60°, 50°)$ up to $K_n = 4$ with all above signals. The number of snapshots is 800 and $M_c = 5000$. As shown in Fig.3 (a) and (b), the estimation performance of

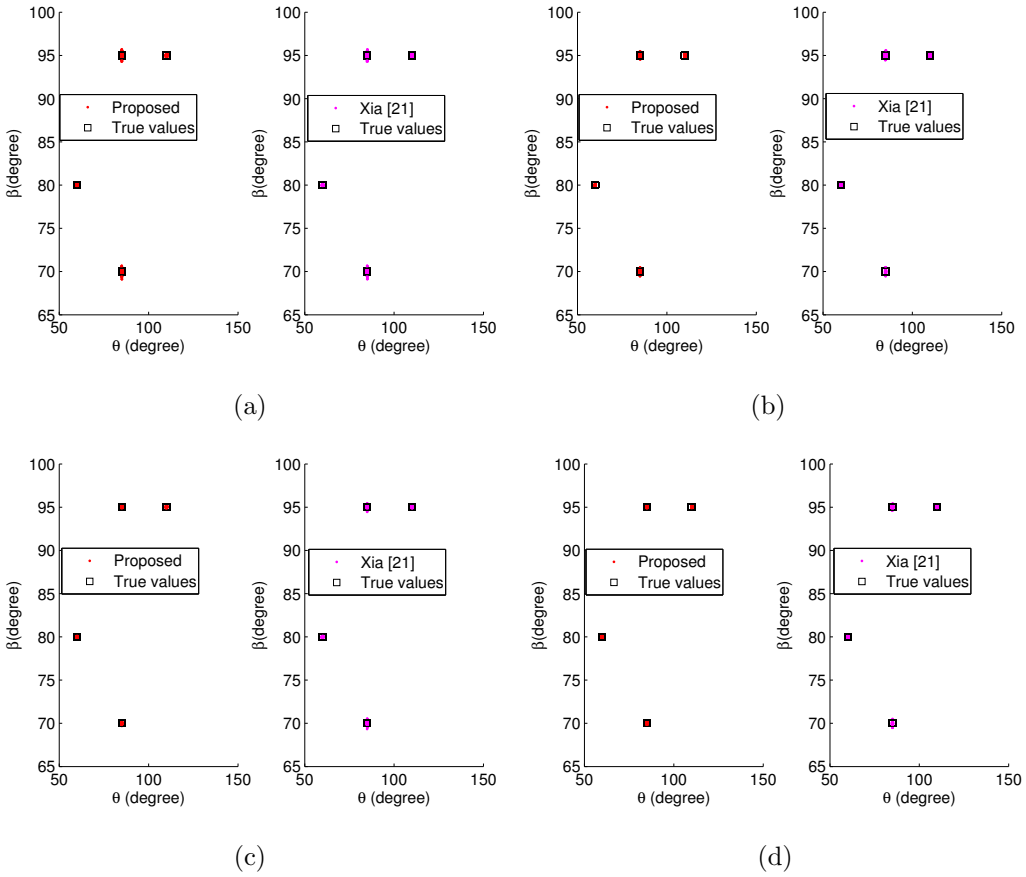

Fig. 2: 2-D scattergram for mixed signals. (a) Case 1: one BPSK and three QPSK signals. (b) Case 2: two BPSK and two QPSK signals. (c) Case 3: three BPSK and one QPSK signals. (d) Case 4: four BPSK signals.

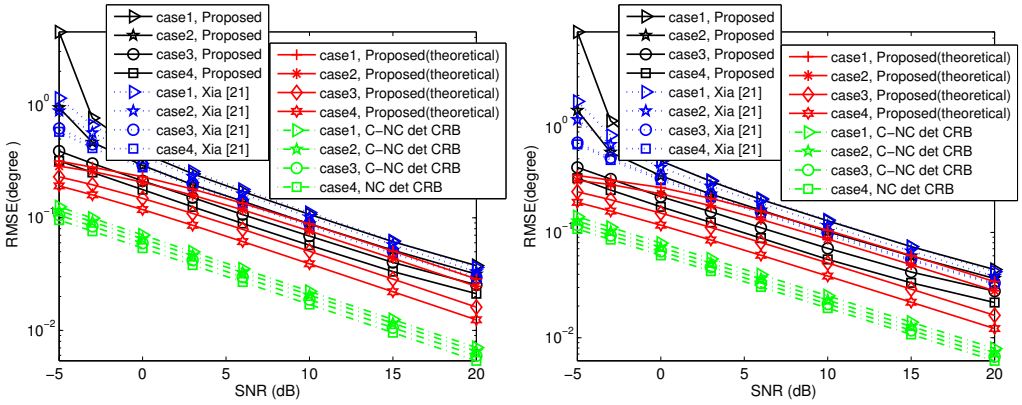

(a) (b)

Fig. 3: RMSE of versus SNR with the number of snapshots to be 800. (a) θ. (b) β.

the proposed method for both angles are superior to that of the method in [21] in all four cases. As before, the performance of the proposed method improves consistently from case 1 to case 4, with more and more noncircularity information available.

6.3. Performance versus snapshots

The performance of the proposed method is studied in this part with the number of snapshots varying from 50 to 1050. The SNR is fixed at 5 dB and the other parameters are the same as in Sec.*6.2*. Simulation results are shown in Fig.4 (a) and (b), and we can draw similar conclusions as in Sec.*6.2*.

6.4. Performance versus angle separation

Now the performance of the proposed method is investigated with the angle separation Δ of 2-D DOAs varying from 0 to 27. The SNR is fixed at 5dB and the snapshot number is 500. Four uncorrelated signals arrive from directions $((60+\Delta)^\circ, (50+\Delta)^\circ)$, $((70+\Delta)^\circ, (50+\Delta)^\circ)$, $((70+\Delta)^\circ, (60+\Delta)^\circ)$

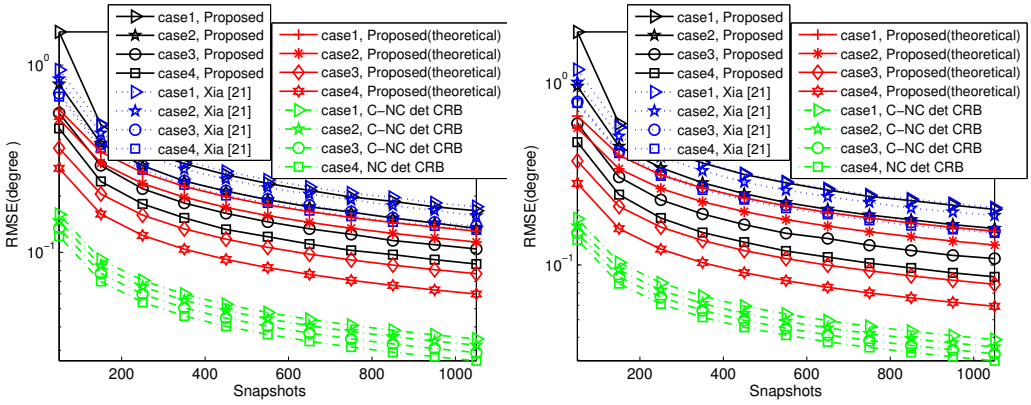

(a) (b)

Fig. 4: RMSE of versus snapshots with SNR fixed at 5dB. (a) θ. (b) β.

and $((80+\Delta)^\circ, (70+\Delta)^\circ)$. We also consider four cases where one, two, three and four BPSK signals are present. Naturally, as angle separation varies from small to large, all methods perform well since the joint diagonalization procedure can solve the angle ambiguity problem, as shown in Fig.5 (a) and (b). Moreover, our proposed method again outperforms the method in [21] for all four cases.

6.5. Performance versus number of rows (columns)

Now we study the effect of array size on the performance. M and N are assigned the same value and vary from 4 to 12. The SNR is fixed at 5dB and the number of snapshot is 800. Fig.6 (a) and (b) show the RMSE of estimated angles obtained by the algorithm in [21] and the proposed one. From case 1 to case 4, it can be seen that the superiority of our proposed algorithm is more significant when the size of array is small such as when the number of rows (columns) equals 4 or 5. When the size of array becomes large in case 1 to case 3, the proposed method is inferior to the method in

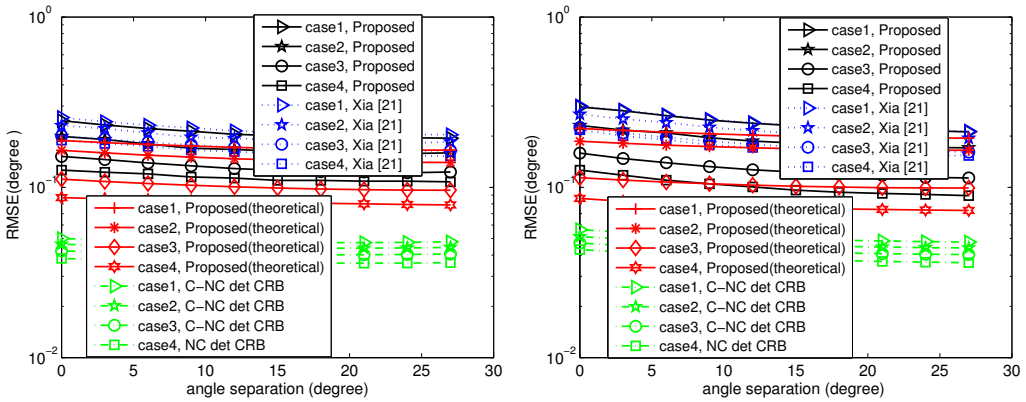

(a) (b)

Fig. 5: RMSE of versus angle separation with SNR fixed at 5dB and the snapshot number to be 500. (a) θ. (b) β.

[21]. This is because when the number of rows (columns) is increased, the size of the new data vector $\tilde{\mathbf{x}}$ becomes larger, and the accuracy of the estimated covariance matrix of $\tilde{\mathbf{x}}$ will be worse with given the number of snapshots. We can improve this phenomenon by increasing the number of snapshots.

7. Conclusion

A 2-D DOA estimation method using the URA has been proposed for a mixture of circular and strictly noncircular signals. Based on an ESPRIT-like method, the estimated 2-D DOAs of the sources are paired automatically by joint diagonalization of two direction matrices. The theoretical error performance of the proposed method is analyzed and a closed-form expression for the deterministic CRB of 2-D DOAs for the mixed signals scenario is derived. Simulation results show that the performance of the proposed method consistently outperforms the reference method that does not exploit the non-

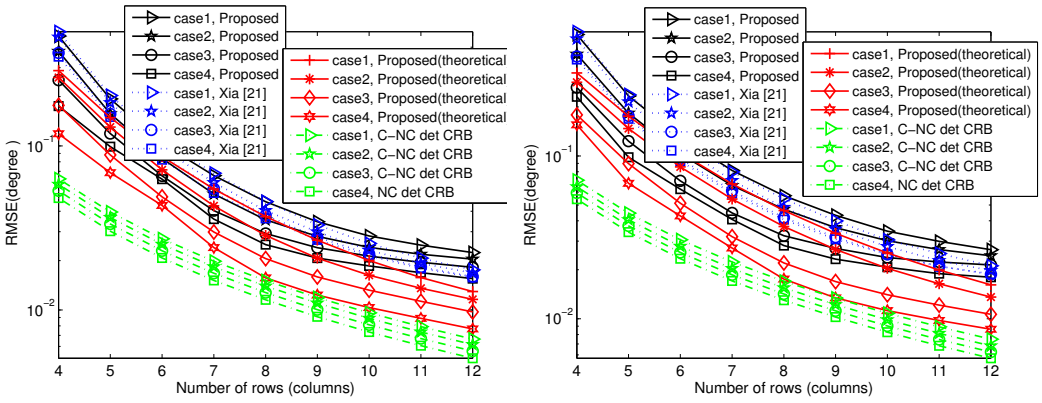

(a) (b)

Fig. 6: RMSE of versus number of rows (columns) with SNR fixed at 5dB and the snapshot number to be 800. (a) θ. (b) β.

circularity information of the impinging signals.

Acknowledgement

This work is supported by the National 863 Programs under Grant (No. 2015AA01A706) and China Scholarship Council (CSC).

[1] H. Krim, M. Viberg,"Two Decades of Array Signal Processing Research-The Parametric Approach," *IEEE Signal Processing Magazine*, vol. 13, no. 4, pp. 67–94, 1996.

[2] A.B. Gershman, M. Rbsamen, M. Pesavento, "One-and two-dimensional direction-of-arrival estimation: An overview of search-free techniques," *Signal Processing*, vol. 90, no. 5, pp. 1338–1349, 2010.

[3] H. Abeida and J.-P. Delmas, "Music-like estimation of direction of ar-

rival for noncircular sources," *IEEE Transactions on Signal Processing*, vol. 54, no. 7, pp. 2678–2690, 2006.

[4] J. Liu, Z. Huang and Y. Zhou, "Extended 2q-MUSIC algorithm for noncircular signals," *Signal Processing*, vol. 88, no. 6, pp. 1327–1339, 2008.

[5] H. Abeida and J.-P. Delmas, "Statistical performance of MUSIC-like algorithms in resolving noncircular sources," *IEEE Transactions on Signal Processing*, vol. 56, no. 9, pp. 4317–4329, 2008.

[6] S. B. Hassen, F. Belliliand, A. Samet and S. Affes, "DOA Estimation of Temporally and Spatially Correlated Narrowband Noncircular Sources in Spatially Correlated White Noise," *IEEE Transactions on Signal Processing*, vol. 59, no. 9, pp. 4108–4121, 2011.

[7] Y. Shi, X. Mao, M. Cao, and Y. Liu, "Deterministic maximum likelihood method for direction-of-arrival estimation of strictly noncircular signals," in *Acoustics, Speech and Signal Processing (ICASSP), 2016 IEEE International Conference on.* IEEE, 2016, pp. 3061–3065.

[8] S. Cao, D. Xu, X. Xu and Z. Ye, "DOA estimation for noncircular signals in the presence of mutual coupling," *Signal Processing*, vol. 105, pp. 12–16, 2014.

[9] J. Liu, Z. Huang, and Y. Zhou, "Azimuth and elevation estimation for noncircular signals," *Electronics letters*, vol. 43, no. 20, pp. 1117–1119, 2007.

[10] L. Gan, J.-F. Gu, and P. Wei, "Estimation of 2-D DOA for noncircular sources using simultaneous svd technique," *IEEE Antennas and Wireless Propagation Letters*, vol. 7, pp. 385–388, 2008.

[11] F. Roemer, and M. Haardt, "Multidimensional unitary Tensor-ESPRIT for Non-Circular sources," in *Acoustics, Speech and Signal Processing (ICASSP), 2009 IEEE International Conference on.* IEEE, 2009, pp. 3577–3580.

[12] J. Steinwandt, F. Roemer, and M. Haardt, "Analytical performance evaluation of multi-dimensional Tensor-ESPRIT-based algorithms for strictly non-circular sources," in *Sensor Array and Multichannel Signal Processing Workshop (SAM), 2016 IEEE International Conference on.* IEEE, 2016.

[13] Y. Shi, L. Huang, C. Qian, and H.C. So, "Direction-of-arrival estimation for noncircular sources via structured least squares-based esprit using three-axis crossed array," *IEEE Transactions on Aerospace and Electronic*, vol. 51, no. 2, pp. 1267–1278, 2015.

[14] J. Steinwandt, F. Roemer, M. Haardt, and G. Del Galdo, "R-dimensional ESPRIT-type algorithms for strictly second-order non-circular sources and their performance analysis," *IEEE Transactions on Signal Processing*, vol. 62, no. 18, pp. 4824–4838, 2014.

[15] J. Steinwandt, F. Roemer, M. Haardt, and G. Del Galdo, "Deterministic Cramer-Rao bound for strictly non-circular sources and analytical anal-

ysis of the achievable gains," *IEEE Transactions on Signal Processing*, vol. 64, no. 17, pp. 4417–4431, 2016.

[16] F. Gao, A. Nallanathan, and Y. Wang, "Improved music under the coexistence of both circular and noncircular sources," *IEEE Transactions on Signal Processing*, vol. 56, no. 7, pp. 3033–3038, 2008.

[17] A. Liu, G. Liao, Q. Xu, and C. Zeng, "A circularity-based doa estimation method under coexistence of noncircular and circular signals," in *Acoustics, Speech and Signal Processing (ICASSP), 2012 IEEE International Conference on.* IEEE, 2012, pp. 2561–2564.

[18] J. Steinwandt, F. Roemer, and M. Haardt, " Esprit-type algorithms for a received mixture of circular and strictly non-circular signals, " in *Acoustics, Speech and Signal Processing (ICASSP), 2015 IEEE International Conference on.* IEEE, 2015, pp. 2809-2813.

[19] Z.-M. Liu, Z.-T. Huang, Y.-Y. Zhou, and J. Liu, "Direction-of-arrival estimation of noncircular signals via sparse representation," *IEEE Transactions on Aerospace and Electronic Systems*, vol. 48, no. 3, pp. 2690–2698, 2012.

[20] H. Chen, C.-P. Hou, W. Liu, W.-P. Zhu and M.N.S. Swamy, "Efficient Two-Dimensional Direction of Arrival Estimation for a Mixture of Circular and Noncircular Sources," *IEEE Sensors Journal*, vol. 16, no. 8, pp. 2527–2536, 2016.

[21] T.Q. Xia, " Joint diagonalization based DOD and DOA estimation for bistatic MIMO radar" *Signal Processing*, vol. 108, pp. 159–166, 2015.

[22] X. Yang, G. Zheng and J. Tang, "ESPRIT algorithm for coexistence of circular and noncircular signals in bistatic MIMO radar" in *IEEE Radar Conference (RadarConf)*, IEEE, 2016, pp. 1-4.

[23] A. Belouchrani, K. Abed-Meraim, J.F. Cardoso, and E. Moulines, " A blind source separation technique using second-order statistics" *IEEE Transactions on Signal Processing*, vol. 45, no. 2, pp. 434–444, 1997.

[24] Y. Y. Dong, C. X. Dong, Y. T. Zhu, G. Q. Zhao,and S. Y. Liu, " Two-dimensional DOA estimation for L-shaped array with nested subarrays without pair matching" *IET Signal Processing*, vol. 10, no. 9, pp. 1112–1117, 2016.

[25] B. D. Rao and K. V. S. Hari, "Performance analysis of ESPRIT and TAM in determining the direction of arrival of plane waves in noise," *IEEE Transactions on acoustics, speech, and signal processing*, vol. 37, no. 12, pp. 1990–1995, 1989.

[26] F. Li, R. J. Vaccaro, and D. W. Tufts, " Performance analysis of the state-space realization (TAM) and ESPRIT algorithms for DOA estimation," *IEEE Transactions on Antennas Propagation*, vol. 39, no. 3, pp. 418–423, 1991.

[27] M. Jin, G. Liao and J. Li, " Joint DOD and DOA estimation for bistatic MIMO radar," *Signal Processing*, vol. 89, no. 2, pp. 244–251, 2009.

[28] Stoica P., Moses R.L., Spectral Analysis of Signals. *Prentice-Hall, NJ*, Appendix B, 285-293, 1997.